

Performance Limits with Additive Error Metrics in Noisy Multi-Measurement Vector Problems

Junan Zhu, *Member, IEEE* and Dror Baron, *Senior Member, IEEE*

Abstract—Real-world applications such as magnetic resonance imaging with multiple coils, multi-user communication, and diffuse optical tomography often assume a linear model where several sparse signals sharing common sparse supports are acquired by several measurement matrices and then contaminated by noise. Multi-measurement vector (MMV) problems consider the estimation or reconstruction of such signals. In different applications, the estimation error that we want to minimize could be the mean squared error or other metrics such as the mean absolute error and the support set error. Seeing that minimizing different error metrics is useful in MMV problems, we study information-theoretic performance limits for MMV signal estimation with arbitrary additive error metrics. We also propose a message passing algorithmic framework that achieves the optimal performance, as verified through numerical examples. As an application of our MMV algorithm, we propose a novel setup for active user detection in multi-user communication and demonstrate the promise of our proposed setup.

Keywords: Active user detection, error metric, message passing, multi-measurement vector problem.

I. INTRODUCTION

Many systems in science and engineering can be approximated by a linear model, where a signal $\mathbf{x} \in \mathbb{R}^N$ is recorded via a measurement matrix $\mathbf{A} \in \mathbb{R}^{M \times N}$, and then contaminated by a measurement channel,

$$\mathbf{w} = \mathbf{A}\mathbf{x}, y_m = \mathcal{Z}(w_m), \forall m \in \{1, \dots, M\}, \quad (1)$$

where $y_m, m \in \{1, \dots, M\}$, are the entries of the measurements $\mathbf{y} \in \mathbb{R}^M$, and the measurement channel $\mathcal{Z}(\cdot)$ is characterized by a probability density function (pdf), $f(y_m|w_m)$. The goal is to estimate \mathbf{x} from the measurements \mathbf{y} given knowledge of \mathbf{A} and a model for the measurement channel $f(y_m|w_m), \forall m$. We call such a system the *single measurement vector (SMV)* problem.

The signal acquisition systems for many applications are distributed, where J measurement matrices measure J different signals individually. The key difference between such a system and J individual SMV's, is that these J signals are somewhat dependent. An example of a model containing such dependencies is the multi-measurement vector (MMV) problem [1–7]. The MMV problem considers the estimation of a set of dependent signals, and has applications such as

magnetic resonance imaging with multiple coils [8, 9], active user detection in multi-user communication [10], and diffuse optical tomography using multiple illumination patterns [5]. In MMV, thanks to the dependencies among different signals, the number of sparse coefficients that can be successfully estimated increases with the number of measurements. This property was evaluated rigorously for noiseless measurements using l_0 minimization [11], if the underlying signals share the same sparse supports. A non-rigorous replica analysis of MMV with measurement noise also shows the benefit of having more signal vectors [12, 13].

Related work: There are many estimation approaches for MMV problems. These include greedy algorithms such as SOMP [1, 14], l_1 convex relaxation [15, 16], and M-FOCUSS [2]. REDUCE MMV and BOOST (ReMBo) has been shown to outperform conventional methods [3], and subspace methods have also been used to solve MMV problems [6, 7]. However, these algorithms cannot handle the case of J different measurement matrices. Statistical approaches [17] often achieve the oracle minimum mean squared error (MMSE). However, when running estimation algorithms for MMV problems, one might be interested in minimizing some other error. For example, if estimating the underlying signal is important, one could use the mean squared error (MSE) metric; when there might be outliers in the estimated signal, using the mean absolute error (MAE) metric might be more appropriate. Seeing that there is no prior work discussing the optimal performance with user-defined error metrics, we study the optimal performance with user-defined additive error metrics in MMV problems where the signals share common sparse supports, and each entry of the measurements is contaminated by parallel measurement channels (i.e., the channel in (1) satisfies $f(\mathbf{y}|\mathbf{w}) = \prod_{m=1}^M f(y_m|w_m)$). Note that a specific error metric, the MSE, has been studied in Zhu et al. [12], which focus on the MSE performance limits (i.e., the MMSE) of MMV signal estimation. In contrast, this work explores performance limits and designs an algorithm that can minimize *arbitrary additive error metrics* beyond MSE.

Contributions: This paper combines insights from Zhu et al. [12] and Tan and coauthors [18, 19], thus yielding a stronger understanding of the MMV problem, which could be extended in future work to other distributed signal acquisition settings, beyond MMV. To be more specific, we make several contributions in this paper. First, by extending Tan and coauthors [18, 19] we provide an algorithm based on a message passing (MP) framework [20, 21] that can be adapted

The work was supported in part by the National Science Foundation under the Grants CCF-1217749 and ECCS-1611112.

Junan Zhu is with J.P.Morgan Chase, NY, NY 10001, and Dror Baron is with the Department of Electrical and Computer Engineering, NC State University, Raleigh, NC 27695. E-mail: {jzhu9, barondror}@ncsu.edu.

to minimize the expected error for arbitrary additive error metrics. Our algorithm first runs MP until MP converges or reaches some stopping criteria, and we then denoise MP's output using a denoiser that minimizes the given additive error metric. Second, we justify that our proposed algorithm indeed achieves the optimal performance, based on Conjecture 1 (Section II-B), which states that MP algorithms for MMV often provide an estimated posterior that converges to the true posterior. Third, as an example, we derive performance limits for MAE and mean weighted support set error (MWSE) by designing the corresponding optimal denoisers, based on the scalar channel noise variance (Section II-B) derived from replica analysis (Appendix B) [12]. Simulation results show the superiority and optimality of our algorithm. We note in passing that having more signal vectors in MMV helps reduce the estimation error. Finally, as an application of MMV and our algorithm, we propose a novel setup for active user detection in multi-user communications (details in Section VI) and demonstrate the promise of our proposed setup through simulation.

Organization: The remainder of the paper is organized as follows. We introduce our problem setting and MP algorithms in Section II. Our algorithmic framework, which can minimize arbitrary additive error metrics, is proposed and justified to be optimal in Section III. For some example error metrics, we derive the corresponding optimal algorithms, together with the theoretical limits for these errors, in Section IV. Synthetic simulation results are discussed in Section V, followed by an application of our metric-optimal algorithm to a real-world problem in Section VI. We conclude in Section VII.

Notations: In this paper, bold capital letters represent matrices, bold lower case letters represent vectors, and normal font letters represent scalars. The m -th entry (scalar) of a vector \mathbf{z} is denoted by z_m .

II. PROBLEM SETTING AND BACKGROUND

A. Problem setting

Signal model: We consider an ensemble of J signal vectors, $\mathbf{x}^{(j)} \in \mathbb{R}^N$, $j \in \{1, \dots, J\}$, where j is the index of the signal. Consider a *super-symbol* $\mathbf{x}_n = [x_n^{(1)}, \dots, x_n^{(J)}]$, $n \in \{1, \dots, N\}$; all super-symbols in this paper are row vectors. The super symbol \mathbf{x}_n follows a J -dimensional distribution,

$$f(\mathbf{x}_n) = \rho \phi(\mathbf{x}_n) + (1 - \rho) \delta(\mathbf{x}_n), \quad (2)$$

where $\rho \in (0, 1)$ determines the percentage of non-zeros in the signal and is called the sparsity rate, $\phi(\mathbf{x}_n)$ is a J -dimensional pdf, and $\delta(\mathbf{x}_n)$ is the delta function for J -dimensional vectors.

Definition 1 (Joint sparsity with common supports): Ensembles of signals are called jointly sparse signals with common sparse supports when they obey (2).

Note that there are other types of joint sparsity [22] that fit into the MMV framework. For example, an MMV model with signal vectors that have slowly changing supports is discussed in Ziniel and Schniter [23]. Since this paper only focuses

on the MMV problem with signals sharing common sparse supports (2), we refer to joint sparsity with common sparse supports as joint sparsity for brevity.

Measurement models: Each signal $\mathbf{x}^{(j)}$ is measured by a measurement matrix $\mathbf{A}^{(j)} \in \mathbb{R}^{M \times N}$ before being corrupted by a random measurement channel,

$$\mathbf{w}^{(j)} = \mathbf{A}^{(j)} \mathbf{x}^{(j)}, \quad y_m^{(j)} = \mathcal{Z}(w_m^{(j)}), \quad (3)$$

$$m \in \{1, \dots, M\}, \quad j \in \{1, \dots, J\},$$

where $y_m^{(j)}, m \in \{1, \dots, M\}$ are the entries of the measurements $\mathbf{y}^{(j)}$, and the measurement channel $\mathcal{Z}(\cdot)$ is characterized by the pdf $f(y_m^{(j)} | w_m^{(j)})$. In this paper, we only focus on independent and identically distributed (i.i.d.) parallel measurement channels, i.e., the pdf's $f(y_m^{(j)} | w_m^{(j)}), \forall m, j$, are identical and there is no cross-talk among different channels; our proposed algorithm is readily extended to parallel channels with different $f(y_m^{(j)} | w_m^{(j)}), \forall m, j$. When the number of signal vectors $J = 1$, we call this MMV model (3) an SMV problem (1).

Definition 2 (Large system limit [24]): The signal length N scales to infinity, and the number of measurements $M = M(N)$ depends on N and also scales to infinity, where the ratio approaches a positive constant R ,

$$\lim_{N \rightarrow \infty} \frac{M(N)}{N} = R > 0.$$

We call R the measurement rate.

For MMV problems, we are given the matrices $\mathbf{A}^{(j)}$ and measurements $\mathbf{y}^{(j)}, \forall j$, as well as knowledge of the measurement channel (3). Our task is to estimate the underlying signal vectors $\mathbf{x}^{(j)}, \forall j$. Suppose that the estimate is $\hat{\mathbf{x}}^{(j)}$. In order to evaluate the quality of the estimate, we define an *additive* error metric for each super-symbol $\hat{\mathbf{x}}_n$ as $d_{\text{UD}}(\mathbf{x}_n, \hat{\mathbf{x}}_n), \forall n$, where the subscript UD (user-defined) means that the error function $d_{\text{UD}}(\cdot)$ can be arbitrarily specified. Therefore, the error of the estimate of the entire signal vectors set $\hat{\mathbf{x}}^{(j)}, \forall j$, is

$$D_{\text{UD}} = \sum_{n=1}^N d_{\text{UD}}(\mathbf{x}_n, \hat{\mathbf{x}}_n).$$

The smaller the D_{UD} is, the better the estimation is.

B. Message passing algorithms

Message passing (MP) algorithms consider a factor graph [20, 21, 25], which expresses the relation between the signals \mathbf{x} and measurements \mathbf{y} . We begin by discussing the factor graph for SMV, followed by that of MMV.

Factor graph for SMV: The left panel of Fig. 1 illustrates the factor graph concept for an SMV problem (1) with i.i.d. entries in the signal \mathbf{x} . The round circles are the variable nodes (representing the distribution of the signal), and the squares denote the factor nodes (representing the measurement channel). The variables $x_n, \forall n$, are driven by each factor node $f(x_n)$ individually, because the signal has i.i.d. entries x_n . The

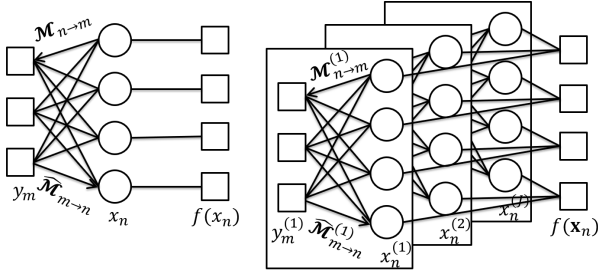


Fig. 1. Factor graph for SMV (left) and MMV (right).

message $\mathcal{M}_{n \rightarrow m}$, passed by the variable node x_n to the factor node y_m , is the pdf of the estimator \hat{x}_n where the variable node x_n is connected to all the factor nodes except for the m -th one. The other message $\hat{\mathcal{M}}_{m \rightarrow n}$, passed by the factor node y_m to the variable node x_n , is the pdf of the estimator \hat{x}_n , where the variable node x_n is only connected to the m -th factor node [21, 25]. The aim of this paper is not the detailed derivation of MP algorithms. Instead, the key property of MP utilized in this paper is that MP converts (1) into the following equivalent scalar channel,

$$\mathbf{q} = \mathbf{x} + \mathbf{v},$$

where \mathbf{q} is the noisy *pseudo data*, and \mathbf{v} is the equivalent scalar channel AWGN whose variance Δ_v can be approximated. After obtaining \mathbf{q} and Δ_v , each variable node x_n updates the estimate \hat{x}_n by denoising q_n . If the signal entries are i.i.d. and the matrix is either i.i.d. or sparse and locally tree-like, then MP algorithms yield a density function $f(x_n|q_n)$ that is statistically equivalent to $f(x_n|\mathbf{y})$ [20].

Factor graph for MMV: An MMV problem with jointly sparse signals can be expressed as the factor graph shown in the right panel of Fig. 1. We can see that the MP in each channel is similar to an SMV problem. The only difference is that the J variable nodes $x_n^{(j)}$, $j \in \{1, \dots, J\}$, for fixed n are driven by one factor node $f(\mathbf{x}_n)$. By grouping the entries from different signal vectors together into super-symbols as in (2), we have i.i.d. super-symbols. The noisy super-symbol pseudo data $\mathbf{q}_n = [q_n^{(1)}, \dots, q_n^{(J)}]$ is denoised, in order to update the estimate for $\mathbf{x}_n = [x_n^{(1)}, \dots, x_n^{(J)}]$. Given the factor graph in Fig. 1, we have the following conjecture.

Conjecture 1: In the large system limit, for the MMV model (3) with signal vectors $\mathbf{x}^{(j)}$ following (2) and locally tree-like sparse measurement matrices or i.i.d. matrices $\mathbf{A}^{(j)}$, MP algorithms with an optimal super-symbol denoiser, $\hat{\mathbf{x}}_n = \mathbb{E}[\mathbf{x}_n|\mathbf{q}_n]$, yield a density function $f(\mathbf{x}_n|\mathbf{q}_n)$ that converges to the posterior $f(\mathbf{x}_n|\{\mathbf{y}^{(j)}\}_{j=1}^J)$, where $\{\mathbf{y}^{(j)}\}_{j=1}^J$ denotes the set $\{\mathbf{y}^{(1)}, \dots, \mathbf{y}^{(J)}\}$.

Conjecture 1 is based on two observations: (i) the measurement channels are i.i.d., so that it suffices to update the estimate of the channel by passing the messages $\mathcal{M}_{n \rightarrow m}^{(j)}$ and $\hat{\mathcal{M}}_{m \rightarrow n}^{(j)}$ for different j individually, and (ii) the super-symbols \mathbf{x}_n are i.i.d., so that denoising each super-symbol individually

Algorithm 1 Metric-optimal algorithm for MMV

- 1: **Inputs:** Measurements $\mathbf{y}^{(j)}$ and matrices $\mathbf{A}^{(j)}, \forall j$
 - 2: **Part 1 (Algorithm 2):** Obtain pseudo data $\mathbf{q}^{(j)}, \forall j$, and scalar channel noise variance Δ_v from MP($\mathbf{y}^{(j)}, \mathbf{A}^{(j)}, \forall j$)
 - 3: **Part 2 (examples in Section IV):** Obtain optimal estimate $\tilde{\mathbf{x}}^{(j)}$ from denoiser using $\mathbf{q}^{(j)}, \Delta_v, \forall j$
 - 4: **Outputs:** $\tilde{\mathbf{x}}^{(j)}, \forall n$
-

accounts for all the information needed to update the estimate. Hence, the MMV factor graph in Fig. 1 leads to Conjecture 1.

III. MAIN RESULTS

Based on Conjecture 1, we first present our metric-optimal algorithm in Section III-A and then in Section III-B we justify that the proposed algorithm is optimal for arbitrary additive error metrics.

A. Achievable part: Metric-optimal estimation algorithm

The metric-optimal algorithm consists of two parts, as illustrated in Algorithm 1. We first run an MP algorithm (Algorithm 2 provides an implementation of an MP algorithm) to get the noisy pseudo data $\mathbf{q}^{(j)}, \forall j$, and the noise variance Δ_v (details below). Next, we denoise $\mathbf{q}^{(j)}, \forall j$, using an optimal denoiser tailored to minimize the given error metric. The following discusses both parts in detail.

MP algorithm: For the first part, we modify the generalized approximate message passing (GAMP) algorithm [20], which is an implementation of MP, and list the pseudo code in Algorithm 2. The notation $\text{diag}(\Theta^{(j)})$ denotes a diagonal matrix whose entries along the diagonal are $\Theta^{(j)}$, $\{\cdot\}^T$ denotes transpose, and the power-of-two in Lines 5 and 12 is applied element-wise. The function g_{out} in Lines 8 and 9 is given by

$$g_{\text{out}}(k, y, \Theta) = \frac{1}{\Theta}(\mathbb{E}[w|k, y, \Theta] - k), \quad (4)$$

where we omit the subscripts and super-scripts for brevity, and the expectation is taken over the pdf,

$$f(w|k, y, \Theta) \propto f(y|w) \exp \left[-\frac{(w - k)^2}{2\Theta} \right]. \quad (5)$$

For the special case of AWGN channels,

$$y = w + z, \quad (6)$$

where $z \sim \mathcal{N}(0, \Delta_z)$, we obtain $g_{\text{out}}(k, y, \Theta) = \frac{y - k}{\Delta_z + \Theta}$ [20]. In Appendix A, we also briefly present the derivation for an i.i.d. parallel logistic channel,

$$f(y|w) = \delta(y - 1) \frac{1}{1 + \exp(-aw)} + \delta(y) \frac{\exp(-aw)}{1 + \exp(-aw)}, \quad (7)$$

where a is a scaling factor.¹

¹Byrne and Schniter [26] describe without detail how to derive $g_{\text{out}}(\cdot)$ (4) for i.i.d. parallel logistic channels (7); we present a detailed derivation for completeness in Appendix A, and do not claim it as a contribution.

Algorithm 2 GAMP for MMV

```

1: Inputs: Maximum number of iterations  $t_{\max}$ , threshold  $\epsilon$ ,
   sparsity rate  $\rho$ , noise variance  $\Delta_z$ , measurements  $\mathbf{y}^{(j)}$ , and
   measurement matrices  $\mathbf{A}^{(j)}, \forall j$ 
2: Initialize:  $t = 1, \delta = \infty, \mathbf{k}^{(j)} = \mathbf{y}^{(j)}, \Theta_m^{(j)} = 0, s_n^{(j)} =$ 
    $\rho\Delta_z, \hat{x}_n^{(j)} = 0, h_m^{(j)} = 0, \forall m, n, j$ 
3: while  $t < t_{\max}$  and  $\delta > \epsilon$  do
4:   for  $j \leftarrow 1$  to  $J$  do
5:      $\Theta^{(j)} = (\mathbf{A}^{(j)})^2 \mathbf{s}^{(j)}$ 
6:      $\mathbf{k}^{(j)} = \mathbf{A}^{(j)} \hat{\mathbf{x}}^{(j)} - \text{diag}(\Theta^{(j)}) \mathbf{h}^{(j)}$ 
7:     for  $m \leftarrow 1$  to  $M$  do
8:        $h_m^{(j)} = g_{\text{out}}(k_m^{(j)}, y_m^{(j)}, \Theta_m^{(j)})$ 
9:        $r_m^{(j)} = -\frac{\partial}{\partial k_m^{(j)}} g_{\text{out}}(k_m^{(j)}, y_m^{(j)}, \Theta_m^{(j)})$ 
10:    end for
11:    // Scalar channel noise variance
12:     $\Delta_v^{(j)} = \left\{ \frac{1}{N} \mathbf{1}^T [(\mathbf{A}^{(j)})^T]^2 \mathbf{r}^{(j)} \right\}^{-1}$ 
13:     $\mathbf{q}^{(j)} = \hat{\mathbf{x}}^{(j)} + \Delta_v^{(j)} (\mathbf{A}^{(j)})^T \mathbf{h}^{(j)}$  // Pseudo data
14:     $\hat{\mathbf{a}}^{(j)} = \hat{\mathbf{x}}^{(j)}$  // Save current estimate
15:  end for
16:   $\Delta_v = \sum_{j=1}^J \Delta_v^{(j)}$ 
17:  for  $n \leftarrow 1$  to  $N$  do
18:     $\hat{\mathbf{x}}_n = f_{a_n}(\Delta_v, \mathbf{q}_n)$  // Estimate
19:     $\mathbf{s}_n = [s_n^{(1)}, \dots, s_n^{(J)}] = f_{v_n}(\Delta_v, \mathbf{q}_n)$  // Variance
20:  end for
21:   $t = t + 1$  // Increment iteration index
22:   $\delta = \frac{1}{NJ} \sum_{n=1}^N \sum_{j=1}^J \left( \hat{x}_n^{(j)} - \hat{a}_n^{(j)} \right)^2$  // Change
23: end while
24: Outputs: Estimate  $\hat{\mathbf{x}}^{(j)}$ , pseudo data  $\mathbf{q}^{(j)}, \forall j$ , and scalar
   channel noise variance  $\Delta_v$ 

```

For the special case of i.i.d. *joint Bernoulli-Gaussian signals* where $\phi(\mathbf{x}_n) \sim \mathcal{N}(0, \mathbb{I})$ in (2) and \mathbb{I} is an identity matrix, f_{a_n} and f_{v_n} in Lines 18 and 19 are given below,

$$f_{a_n}(\Delta_v, \mathbf{q}_n) = \frac{\rho}{C(\Delta_v + 1)} \mathbf{q}_n, \quad (8)$$

$$f_{v_n}(\Delta_v, \mathbf{q}_n) = -[f_{a_n}(\Delta_v, \mathbf{q}_n)]^2 + \frac{\rho}{C(\Delta_v + 1)} \left[\frac{\mathbf{q}_n^2}{\Delta_v + 1} + \Delta_v \right],$$

where $\mathbf{q}_n^2 = \left[(q_n^{(1)})^2, \dots, (q_n^{(J)})^2 \right]$ and

$$C = \rho + (1 - \rho) \left(1 + \frac{1}{\Delta_v} \right)^{\frac{J}{2}} \exp \left[-\frac{\mathbf{q}_n \mathbf{q}_n^T}{2\Delta_v(\Delta_v + 1)} \right].$$

Notice that in Line 12 we take the mean of a vector to obtain a scalar $\Delta_v^{(j)}$, which is the average of the variances for the estimates of signal entries $x_n^{(j)}$. This is because the super-symbols $\mathbf{x}_n, \forall n$, of the signals are i.i.d and the J measurement channels are i.i.d. For the same reason, $\Delta_v^{(j)}, j \in \{1, \dots, J\}$, should be close to each other; hence, Line 16. Note that Algorithm 2 assumes that the entries of $\mathbf{A}^{(j)}$ scale with $\frac{1}{\sqrt{N}}$,

and is a more generic form of an algorithm from our prior work with Krzakala [12].

Metric-optimal denoiser: The second part of our metric-optimal algorithm takes as inputs the noisy pseudo data $\mathbf{q}_n = \mathbf{x}_n + \mathbf{v}_n$ and the estimated variance of \mathbf{v}_n , Δ_v , from the MP algorithm. Using Bayes' rule, we can derive the posterior $f(\mathbf{x}_n | \mathbf{q}_n)$ and use $f(\mathbf{x}_n | \mathbf{q}_n)$ to formulate the optimal estimator in the sense of the user-defined error metric. The optimal estimate is

$$\tilde{\mathbf{x}}_n = \arg \min_{\tilde{\mathbf{x}}_n} \int d_{\text{UD}}(\mathbf{x}_n, \tilde{\mathbf{x}}_n) f(\mathbf{x}_n | \mathbf{q}_n) d\mathbf{x}_n. \quad (9)$$

B. Converse part: The optimal estimate

Algorithm 1 provides us with an estimate $\tilde{\mathbf{x}}_n$; in this section, we justify that $\tilde{\mathbf{x}}_n$ is optimal based on Conjecture 1.

Conjecture 2: In the large system limit, for the MMV model (3) with the signal in (2) and the user-defined additive error metric $d_{\text{UD}}(\mathbf{x}_n, \tilde{\mathbf{x}}_n)$, the optimal estimate of the signal vectors is

$$\tilde{\mathbf{x}}_n = \arg \min_{\tilde{\mathbf{x}}_n} \mathbb{E}[d_{\text{UD}}(\mathbf{x}_n, \tilde{\mathbf{x}}_n) | \mathbf{q}_n].$$

To justify Conjecture 2, recall that the optimal estimate of each super-symbol \mathbf{x}_n in the signal vectors is

$$\tilde{\mathbf{x}}_{\text{true}, n} = \arg \min_{\tilde{\mathbf{x}}_n} \int d_{\text{UD}}(\mathbf{x}_n, \tilde{\mathbf{x}}_n) f(\mathbf{x}_n | \{\mathbf{y}^{(j)}\}_{j=1}^J) d\mathbf{x}_n. \quad (10)$$

Comparing (9) and (10), given that the density function $f(\mathbf{x}_n | \mathbf{q}_n)$ converges to the posterior $f(\mathbf{x}_n | \{\mathbf{y}^{(j)}\}_{j=1}^J)$ (Conjecture 1), we have

$$\tilde{\mathbf{x}}_n = \arg \min_{\tilde{\mathbf{x}}_n} \mathbb{E}[d_{\text{UD}}(\mathbf{x}_n, \tilde{\mathbf{x}}_n) | \mathbf{q}_n] \approx \tilde{\mathbf{x}}_{\text{true}, n},$$

which justifies Conjecture 2.

IV. EXAMPLE METRIC-OPTIMAL ESTIMATORS AND PERFORMANCE LIMITS

In order to derive metric-optimal estimators, we need to know the scalar channel noise variance, Δ_v . Below we obtain the optimal estimator, which is then used as part of Algorithm 1 and to evaluate the performance limits of our metric-optimal algorithm.

For i.i.d. matrices and AWGN channels (6), replica analysis in our previous work with Krzakala [12] yields the information-theoretic scalar channel noise variance Δ_v for message passing algorithms, which characterizes the posterior $f(\mathbf{x}_n | \mathbf{q}_n)$.² Hence, we can obtain the information-theoretic optimal performance with arbitrary additive error metrics. For other types of matrices that satisfy the assumptions of Conjecture 1, our replica analysis [12] does not hold. Nevertheless, MP algorithms still yield a posterior $f(\mathbf{x}_n | \mathbf{q}_n)$, which

²Our work with Krzakala [12] focuses on a diagonal covariance matrix for \mathbf{x}_n in (2). A recent work by Hannak et al. [27] extends our work [12] to non-diagonal covariance matrices for \mathbf{x}_n . Following Hannak et al. [27], we can extend the performance limits analysis in this paper to non-diagonal covariance matrices for \mathbf{x}_n .

according to Conjecture 1 converges to the true posterior $f(\mathbf{x}_n|\{\mathbf{y}^{(j)}\}_{j=1}^J)$. Hence, we can still assume that the scalar channel noise variance Δ_v is known. Based on the known variance Δ_v , we build metric-optimal estimators for two examples, mean weighted support set error (Section IV-A) and mean absolute error (Section IV-B).

A. Mean weighted support set error (MWSE)

MWSE-optimal estimator: In support set estimation, the goal is to estimate the support of the signal, which is 1 if the corresponding entry in the signal is non-zero and 0 if it is zero. There are two types of errors in support set estimation: false alarms (support is 0, but estimated to be 1) and misses (support is 1, but estimated to be 0). In some applications such as medical imaging and radar detection, a miss may mean that the doctor misses an illness of the patient, or the radar misses an incoming missile. Hence, the cost paid for a miss could be tremendous compared to a false alarm. There are other applications where a false alarm is more costly than a miss. For example, in court, if an innocent person is mistakenly judged guilty, he/she will likely suffer a great deal. Therefore, we should weight these two errors differently in different applications. Let b_n and \hat{b}_n be the true support and the estimated support of the n -th entry of the signal, respectively, and $\beta \in [0, 1]$ is an application-dependent weight, which reflects the trade-off between the false alarms and misses. Hence, the MWSE given the pseudo data \mathbf{q}_n is

$$\text{MWSE}|\mathbf{q}_n = \mathbb{E}[d_{\text{WSE}}(b_n, \hat{b}_n)|\mathbf{q}_n] = \begin{cases} (1-\beta) \Pr(b_n = 1|\mathbf{q}_n), & \hat{b}_n = 0 \text{ and } b_n = 1, \\ \beta \Pr(b_n = 0|\mathbf{q}_n), & \hat{b}_n = 1 \text{ and } b_n = 0, \\ 0, & \hat{b}_n = b_n, \end{cases} \quad (11)$$

where $\Pr(\cdot)$ denotes probability. The optimal estimate \tilde{b}_n minimizes $\mathbb{E}[d_{\text{WSE}}(b_n, \tilde{b}_n)|\mathbf{q}_n]$ (11), which implies

$$\tilde{b}_n = \begin{cases} 0, & (1-\beta) \Pr(b_n = 1|\mathbf{q}_n) \leq \beta \Pr(b_n = 0|\mathbf{q}_n), \\ 1, & (1-\beta) \Pr(b_n = 1|\mathbf{q}_n) > \beta \Pr(b_n = 0|\mathbf{q}_n). \end{cases} \quad (12)$$

Since $f(\mathbf{q}_n|b_n = 0) = (2\pi\Delta_v)^{-\frac{J}{2}} \exp\left(-\frac{\mathbf{q}_n\mathbf{q}_n^T}{2\Delta_v}\right)$ and $f(\mathbf{q}_n|b_n = 1) = [2\pi(\Delta_v + 1)]^{-\frac{J}{2}} \exp\left[-\frac{\mathbf{q}_n\mathbf{q}_n^T}{2(\Delta_v + 1)}\right]$, we have

$$\Pr(b_n = 1|\mathbf{q}_n) = \frac{\frac{\rho}{[2\pi(1+\Delta_v)]^{\frac{J}{2}}} e^{-\frac{\mathbf{q}_n\mathbf{q}_n^T}{2(1+\Delta_v)}}}{\frac{\rho}{[2\pi(1+\Delta_v)]^{\frac{J}{2}}} e^{-\frac{\mathbf{q}_n\mathbf{q}_n^T}{2(1+\Delta_v)}} + \frac{(1-\rho)}{(2\pi\Delta_v)^{\frac{J}{2}}} e^{-\frac{\mathbf{q}_n\mathbf{q}_n^T}{2\Delta_v}}},$$

and $\Pr(b_n = 0|\mathbf{q}_n) = 1 - \Pr(b_n = 1|\mathbf{q}_n)$. Plugging $\Pr(b_n = 1|\mathbf{q}_n)$ and $\Pr(b_n = 0|\mathbf{q}_n)$ into (12), we have

$$\tilde{b}_n = \begin{cases} 0, & \mathbf{q}_n\mathbf{q}_n^T \leq \tau, \\ 1, & \mathbf{q}_n\mathbf{q}_n^T > \tau, \end{cases} \quad (13)$$

where $\tau = 2\Delta_v(1 + \Delta_v) \ln \left[\frac{\beta(1-\rho)}{(1-\beta)\rho} \left(\frac{1+\Delta_v}{\Delta_v} \right)^{\frac{J}{2}} \right]$, and we remind the reader that ρ is the sparsity rate.

Performance limits: Utilizing (13) and taking expectation over the pseudo data \mathbf{q}_n for $\mathbb{E}[d_{\text{WSE}}(b_n, \hat{b}_n)|\mathbf{q}_n]$ (11), we obtain the minimum MWSE (MMWSE),

$$\begin{aligned} \text{MMWSE} &= \mathbb{E}[d_{\text{WSE}}(b_n, \tilde{b}_n)] \\ &= \int_{\mathbf{q}_n\mathbf{q}_n^T > \tau} \beta \Pr(b_n = 0|\mathbf{q}_n) f(\mathbf{q}_n) d\mathbf{q}_n + \\ &\quad \int_{\mathbf{q}_n\mathbf{q}_n^T \leq \tau} (1-\beta) \Pr(b_n = 1|\mathbf{q}_n) f(\mathbf{q}_n) d\mathbf{q}_n. \end{aligned} \quad (14)$$

We have two integrals to simplify in (14), where we show the first below, and the second can be obtained similarly. To derive the first integral, note that

$$\int_{\mathbf{q}_n\mathbf{q}_n^T > \tau} \Pr(b_n = 0|\mathbf{q}_n) f(\mathbf{q}_n) d\mathbf{q}_n = \Pr(\mathbf{q}_n\mathbf{q}_n^T > \tau, b_n = 0). \quad (15)$$

Next, we calculate the pdf of the random variable (RV) $g_n = \frac{\mathbf{q}_n\mathbf{q}_n^T}{\Delta_v}$ given $b_n = 0$. Because the entries of \mathbf{q}_n are i.i.d. $\mathcal{N}(0, \Delta_v)$ given $b_n = 0$, g_n follows the Chi-square distribution, $f_G(g_n) = \frac{g_n^{\frac{J}{2}-1} \exp(-\frac{g_n}{2})}{2^{\frac{J}{2}} \Gamma(\frac{J}{2})}$, where $\Gamma(\cdot)$ is the Gamma function. Let $r_n = \Delta_v g = \mathbf{q}_n\mathbf{q}_n^T$, then we obtain

$$f(r_n) = \frac{1}{\Delta_v} f_G\left(\frac{r_n}{\Delta_v}\right) = \frac{r_n^{\frac{J}{2}-1} \exp\left[-\frac{r_n}{2\Delta_v}\right]}{(2\Delta_v)^{J/2} \Gamma(J/2)},$$

which helps to simplify (15). Therefore, (14) can be simplified,

$$\begin{aligned} \text{MMWSE} &= \beta(1-\rho) \underbrace{\int_{r_n=\tau}^{\infty} \frac{r_n^{\frac{J}{2}-1} \exp\left[-\frac{r_n}{2\Delta_v}\right]}{(2\Delta_v)^{J/2} \Gamma(J/2)} dr_n}_{\text{Pr(false alarm)}} \\ &\quad + (1-\beta)\rho \underbrace{\int_{r_n=0}^{\tau} \frac{r_n^{\frac{J}{2}-1} \exp\left[-\frac{r_n}{2(1+\Delta_v)}\right]}{[2(1+\Delta_v)]^{J/2} \Gamma(J/2)} dr_n}_{\text{Pr(miss)}}. \end{aligned} \quad (16)$$

Hamming distance: In digital wireless communication systems, the signal only takes discrete values. A useful error metric is the (per-entry) Hamming distance [28], which equals 1 if the estimate of an entry of the signal differs from the true value. (Section VI will present an example in wireless communication that minimizes the Hamming distance.) The reader can verify that Hamming distance can be interpreted as a special case of weighted support set error, where $\beta = 0.5$ provides equal weight to both errors (11). That said, we provide more insights about this particular case, which is ubiquitous in communication systems.

For the jointly sparse model in (2), we define the Hamming distance as

$$d_{\text{HD}}(\mathbf{x}_n, \hat{\mathbf{x}}_n) = \mathbb{1}_{\mathbf{x}_n \neq \hat{\mathbf{x}}_n}, \quad (17)$$

where $\mathbb{1}_{\mathcal{A}}$ is the indicator function. If (i) the pdf $\phi(\mathbf{x}_n)$ in (2) is a J -dimensional Dirac-delta function $\delta(\mathbf{x}_n - \mathbf{1})$, where $\mathbf{1}$ is an all-one row vector, and (ii) the estimate satisfies $\hat{x}_n^{\{1\}} = \dots = \hat{x}_n^{\{J\}}, \forall n \in \{1, \dots, N\}$, then the weighted support set

error (11) with weight $\beta = 0.5$ is equal to half of the Hamming distance (17) for super symbols. In (18)–(19), we briefly derive the Hamming distance-optimal estimator when $\mathbf{x}_n \in \{\mathbf{1}, \mathbf{0}\}$, where $\mathbf{0}$ is an all-zero row vector. The mean Hamming distance (MHD) given the pseudo data \mathbf{q}_n is

$$\text{MHD}|\mathbf{q}_n = \mathbb{E}[d_{\text{MHD}}(\mathbf{x}_n, \hat{\mathbf{x}}_n)|\mathbf{q}_n] = \begin{cases} \Pr(\mathbf{x}_n = \mathbf{1}|\mathbf{q}_n), & \hat{\mathbf{x}}_n = \mathbf{0} \text{ and } \mathbf{x}_n = \mathbf{1}, \\ \Pr(\mathbf{x}_n = \mathbf{0}|\mathbf{q}_n), & \hat{\mathbf{x}}_n = \mathbf{1} \text{ and } \mathbf{x}_n = \mathbf{0}, \\ 0, & \hat{\mathbf{x}}_n = \mathbf{x}_n. \end{cases} \quad (18)$$

Following the steps in (12)–(13), the minimum MHD (MMHD) estimator is

$$\tilde{\mathbf{x}}_n = \begin{cases} \mathbf{1}, & \sum_{j=1}^J q_n^{(j)} \geq \frac{J}{2} + \Delta_v \ln \left[\frac{1-\rho}{\rho} \right], \\ \mathbf{0}, & \sum_{j=1}^J q_n^{(j)} < \frac{J}{2} + \Delta_v \ln \left[\frac{1-\rho}{\rho} \right]. \end{cases} \quad (19)$$

B. Mean absolute error (MAE)

MAE-optimal estimator: The element-wise absolute error (AE) is

$$d_{\text{AE}}(x_n^{(j)}, \hat{x}_n^{(j)}) = |x_n^{(j)} - \hat{x}_n^{(j)}|. \quad (20)$$

In order to find the minimum mean absolute error (MMAE) estimate, $\tilde{\mathbf{x}}_n$, we need to find the stationary point of (20),

$$\left. \frac{d\mathbb{E}[|x_n^{(j)} - \hat{x}_n^{(j)}| | \mathbf{q}_n]}{d\hat{x}_n^{(j)}} \right|_{\hat{x}_n^{(j)} = \tilde{x}_n^{(j)}} = 0, \quad (21)$$

$\forall j \in \{1, \dots, J\}, n \in \{1, \dots, N\}$. It can be proved that $\mathbb{E}[X] = \int_0^\infty \Pr(X > x)dx$, if $X \geq 0$. Therefore,

$$\begin{aligned} \mathbb{E}[|x_n^{(j)} - \hat{x}_n^{(j)}| | \mathbf{q}_n] &= \int_0^\infty \Pr(|x_n^{(j)} - \hat{x}_n^{(j)}| > t | \mathbf{q}_n) dt \\ &= \int_{-\infty}^{\hat{x}_n^{(j)}} \Pr(x_n^{(j)} < t | \mathbf{q}_n) dt + \int_{\hat{x}_n^{(j)}}^\infty \Pr(x_n^{(j)} > t | \mathbf{q}_n) dt. \end{aligned} \quad (22)$$

Using (21) and (22), we obtain

$$\Pr(x_n^{(j)} < \tilde{x}_n^{(j)} | \mathbf{q}_n) = \Pr(x_n^{(j)} > \tilde{x}_n^{(j)} | \mathbf{q}_n).$$

That is,

$$\int_{-\infty}^{\tilde{x}_n^{(j)}} f(x_n^{(j)} | \mathbf{q}_n) dx_n^{(j)} = \int_{\tilde{x}_n^{(j)}}^\infty f(x_n^{(j)} | \mathbf{q}_n) dx_n^{(j)} = \frac{1}{2},$$

through which we solve for the optimal estimator $\tilde{x}_n^{(j)}$ numerically.

Performance limits: We calculate the MMAE as follows,

$$\begin{aligned} \text{MMAE} &= \mathbb{E}[|\tilde{x}_n^{(j)} - x_n^{(j)}|] = \int_{-\infty}^\infty \mathbb{E}[|\tilde{x}_n^{(j)} - x_n^{(j)}| | \mathbf{q}_n] f(\mathbf{q}_n) d\mathbf{q}_n \\ &= \int_{-\infty}^\infty \left[\int_{-\infty}^{\tilde{x}_n^{(j)}} -x_n^{(j)} f(x_n^{(j)} | \mathbf{q}_n) dx_n^{(j)} + \int_{\tilde{x}_n^{(j)}}^\infty x_n^{(j)} f(x_n^{(j)} | \mathbf{q}_n) dx_n^{(j)} \right] f(\mathbf{q}_n) d\mathbf{q}_n, \end{aligned} \quad (23)$$

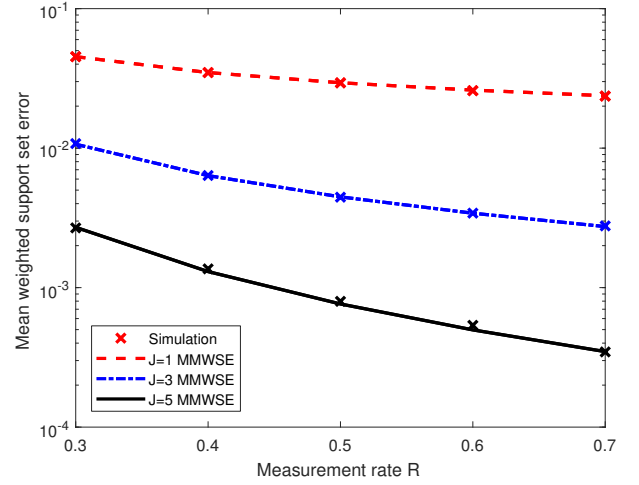


Fig. 2. Comparison of simulation results to theoretic MMWSE for weighted support set estimation under different number of channels J and measurement rates R ($\beta = 0.2$, noise variances $\Delta_z = 0.01$).

which has to be numerically approximated.

V. SYNTHETIC SIMULATIONS

After deriving the minimum mean weighted support set error (MMWSE) and minimum mean absolute error (MMAE) estimators, this section provides numerical results for Algorithm 1. In the case of i.i.d. random matrices and AWGN channels (6), replica analysis yields the MMSE of the MMV problem [12]. By inverting the MMSE (details in Appendix B), we obtain the scalar channel noise variance Δ_v ,³ which characterizes the posterior $f(\mathbf{x}_n | \mathbf{q}_n)$. Given Δ_v , we characterize the MMWSE and MMAE theoretically. In the following simulations, we use i.i.d. Gaussian matrices with unit-norm rows, i.i.d. J -dimensional Bernoulli-Gaussian signals (2) with $J = 1, 3$, and 5 , and sparsity rate $\rho = 0.1$. The signal length is $N = 10000$, and the measurement rate $R = \frac{M}{N}$ varies from 0.3 to 0.7 . For each setting, the simulation results are averaged over 50 realizations of the problem.

Mean weighted support set error in AWGN channels: We simulate AWGN channels (6) in this case with the noise variance being $\Delta_z \in \{0.01, 0.001\}$. Fig. 2 shows the weighted support set estimation results using our metric-optimal algorithm compared to the MMWSE (16). The curves plot the MMWSE and the crosses represent the simulation results. Different colors and line shapes refer to different J 's. We can see that our simulation results match the theoretically optimal performance.

³Algorithm 1 also applies to problems with other types of matrices, as long as the matrices satisfy the condition in Conjecture 1 and the entries in the measurement matrices scale with $\frac{1}{\sqrt{N}}$. However, when the matrices are not i.i.d., there is no easy way to *theoretically* characterize the MMSE, the equivalent scalar channel noise variance Δ_v , and the metric-optimal error. Such a theoretic characterization is sometimes necessary, because the MMSE behaves differently under different noise variances Δ_z (6) and measurement rates R [12, 29].

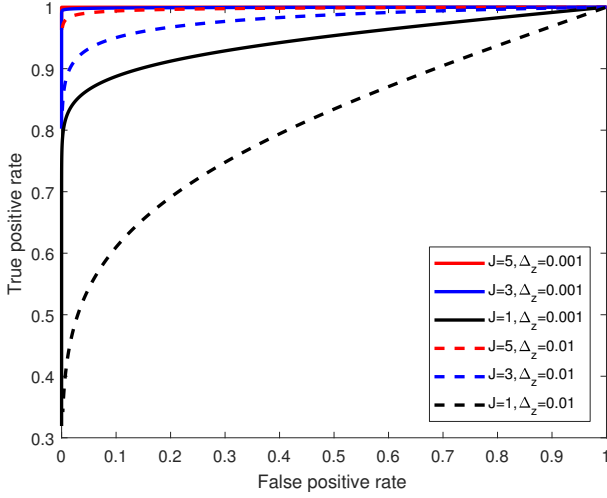


Fig. 3. Receiver operating characteristic curves for weighted support set estimation under different channel noise variances Δ_z and number of channels J ($\beta = 0.2$, measurement rate $R = 0.3$).

For weighted support set estimation, we further study the information-theoretic optimal receiver operating characteristic (ROC) curves, which are plotted in Fig. 3 for different J 's. The solid curves and dashed curves are plotted for noise variances $\Delta_z = 0.001$ and 0.01 , respectively. Different colors represent different values of J . The true positive rate (TPR) and false positive rate (FPR) in both axes are defined as $\text{TPR} = \frac{\# \text{ accurately predicted positives}}{\# \text{ all positives in truth}}$ and $\text{FPR} = \frac{\# \text{ wrongly predicted negatives}}{\# \text{ all negatives in truth}}$. We can see that having more signal vectors J leads to more area under the ROC curve, which indicates better trade-offs between true positives and false positives.

Mean absolute error in logistic channels: We simulate i.i.d. logistic channels (7) with parameters $a = 10$ and 30 ; the smaller a is, the noisier the channel becomes. Fig. 4 plots the simulated MAE (crosses) and the theoretic MMAE (23) (curves) for various settings.⁴ Different colors and line shapes refer to different J 's and a 's, respectively. We can see that our simulation results match the theoretically optimal performance.

Remark: Both simulations yield better performance for larger J . This is intuitive, because more signal vectors that share the same support should make the estimation process easier due to more information being available.

VI. APPLICATION

In this section, we discuss active user detection (AUD) in a multi-user communication setting that can be viewed as compressed sensing [30–32] (CS, which is closely related to SMV) in some scenarios. Next, we simulate AUD using our metric-optimal algorithm. Finally, we solve the AUD problem with an MMV setting.

⁴We do not have a replica analysis for logistic channels. In order to compute the theoretic MMAE, we use the average Δ_v from all the 50 simulations for each setting and calculate the MMAE with (23).

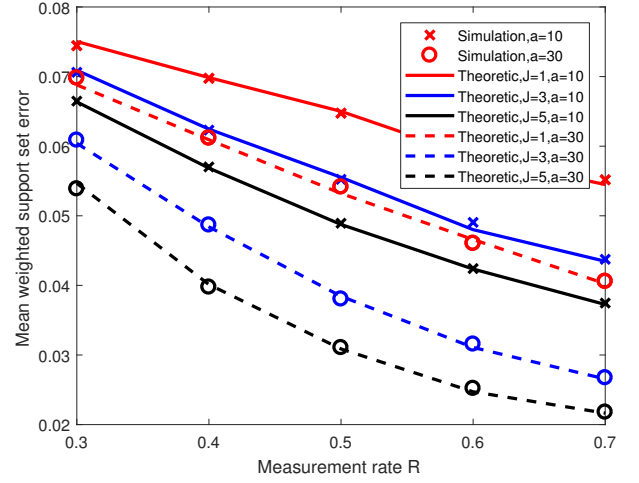


Fig. 4. Comparison of simulation results to theoretic MMAE under different logistic channels (7), number of channels J , and measurement rates R .

CS based active user detection: One application of MMV is AUD in a massive random access (MRA) scenario for multi-user communication [10]. In the MRA scenario, multiple end users (EUs) are requesting access to the network simultaneously by sending their unique identification codewords, $\mathbf{a}_n \in \{-1, +1\}^{M \times 1}$, $n \in \{1, \dots, N\}$, to the base station, where n denotes the user id, and each user's codeword is known by the base station. The base station needs to determine which EUs are requesting access to the network (active) and which are not (inactive), so that it can allocate resources to the active EUs. Boljanović et al. [10] proposed a CS based AUD scheme for MRA. In their setup [10], all EUs are synchronized, i.e., all active EUs send their codewords to the base station simultaneously in one time slot. Denote the status of the n -th EU by $x_n \in \{0, 1\}$, where $x_n = 1$ means active and $x_n = 0$ is inactive. Denote the received signal vector at the base station by $\mathbf{y} \in \mathbb{R}^{M \times 1}$. Since all EUs are synchronized, we can express the received signal \mathbf{y} by

$$\mathbf{y} = \mathbf{A}\mathbf{x} + \mathbf{z}, \quad (24)$$

where $\mathbf{A} = [\mathbf{a}_1, \dots, \mathbf{a}_N] \in \{0, 1\}^{M \times N}$, and \mathbf{z} is AWGN. The base station estimates \mathbf{x} to determine which EUs are active.

In the following, we first apply a mean Hamming distance (MHD) optimal algorithm to estimate \mathbf{x} from (24), and compare to the algorithm of Boljanović et al. [10], which is orthogonal match pursuit (OMP) [33]. Next, we propose an MMV based scheme for AUD in MRA.

Simulation with MHD-optimal algorithm: As the reader can see, the scheme proposed by Boljanović et al. [10] is an SMV problem (1), which is MMV for $J = 1$ (3). Later in this section we will extend the scheme by Boljanović et al. to an MMV setting, and so we keep using MMV notations. Note that the entries of the measurement matrix in this AUD problem take values of ± 1 . Because the derivation of Algorithm 2

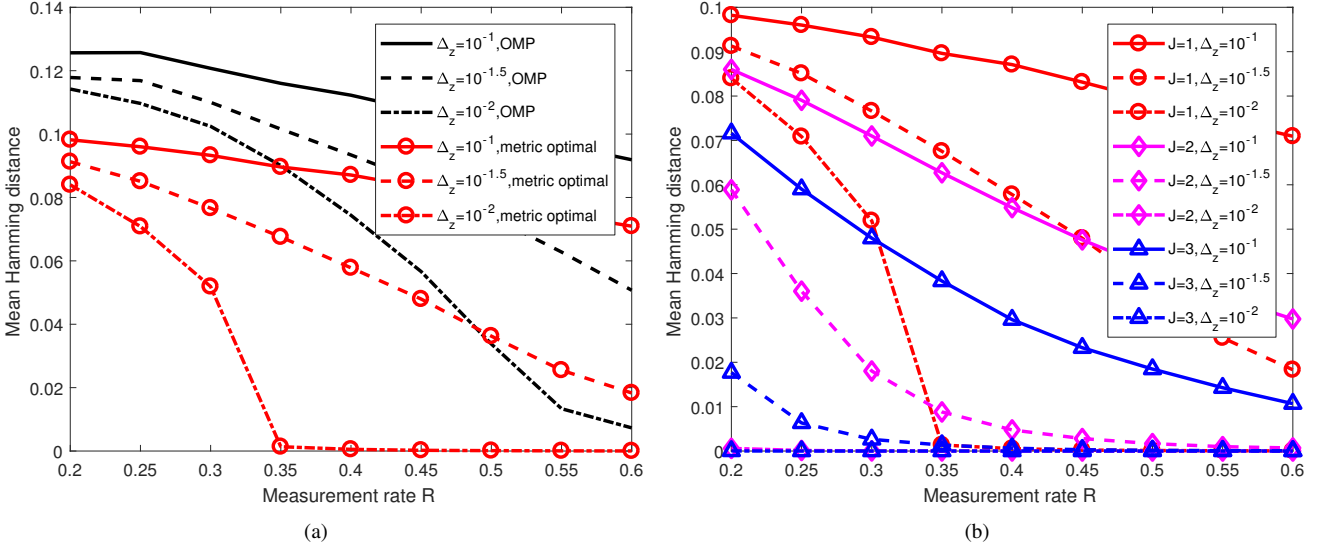


Fig. 5. Simulation results for active user detection in multi-user communication. (a) OMP vs. Algorithm 1 when $J = 1$ and (b) Algorithm 1 when $J = 1, 2, 3$.

assumes that entries of $\mathbf{A}^{(j)}$ scale with $\frac{1}{\sqrt{N}}$,⁵ we scale $\mathbf{A}^{(j)}$ down by \sqrt{N} using a modified $\tilde{\mathbf{y}}^{(j)} = \frac{\mathbf{y}^{(j)}}{\sqrt{N}}$ (1).

Following the discussion above, we simulate the settings of measurement rate $R \in \{0.2, 0.25, \dots, 0.6\}$ and noise variance $\Delta_z \in \{10^{-1}, 10^{-1.5}, 10^{-2}\}$. For each setting, we randomly generate 50 realizations of the Bernoulli signal $\mathbf{x}^{(1)} \in \{0, 1\}^{N \times 1}$ with sparsity rate $\rho = 0.1$, and measurement matrix $\mathbf{A}^{(1)} \in \left\{ -\frac{1}{\sqrt{N}}, +\frac{1}{\sqrt{N}} \right\}^{M \times N}$, where $N = 10000$. We run Algorithm 1 with $J = 1$ to estimate the underlying signal $\mathbf{x}^{(1)}$. Note that $f_{a_n}(\Delta_v, \mathbf{q}_n)$ and $f_{v_n}(\Delta_v, \mathbf{q}_n)$ in Lines 18–19 of Algorithm 2, which consists of Part 2 of Algorithm 1, are given by the following,

$$f_{a_n}(\Delta_v, \mathbf{q}_n) = \frac{\rho}{\rho + (1 - \rho) \exp \left[-\frac{\sum_{j=1}^J q_n^{(j)} - \frac{J}{2}}{\Delta_v} \right]} \mathbf{1},$$

$$f_{v_n}(\Delta_v, \mathbf{q}_n) = f_{a_n}(\Delta_v, \mathbf{q}_n) - f_{a_n}(\Delta_v, \mathbf{q}_n)^2,$$

where the power-of-two in the last term of $f_{v_n}(\cdot, \cdot)$ is applied element-wise.

Our results are compared to OMP in Fig. 5(a). The solid, dashed, and dash-dotted curves represent noise variance $\Delta_z = 10^{-1}$, $10^{-1.5}$, and 10^{-2} , respectively. The black curves are the OMP results and the red curves with circle markers are the results of Algorithm 1 when optimizing for MHD. We can see that our algorithm consistently outperforms OMP.⁶

MMV scheme for active user detection: Reminiscing on Section V and our previous work with Krzakala on MMV [12], more measurement vectors (larger J) lead to better estimation quality. We propose to convert the SMV style of the AUD

problem into an MMV style by having each EU send J different identification codewords, $\mathbf{a}_n^{(j)} \in \{-1, +1\}^{M \times 1}, \forall j \in \{1, \dots, J\}$, to the base station. Fig. 5(b) shows the results of using $J = 1, 2$ and 3 codewords for each EU. Since we are not aware of any algorithm that can deal with different measurement matrices $\mathbf{A}^{(j)}, j \in \{1, \dots, J\}$, with jointly sparse signals, we only plot our results in Fig. 5(b). The solid, dashed, and dash-dotted curves represent different noise variance Δ_z . The red curves with circle markers, the magenta curves with diamond markers, and the blue curves with triangle markers are the results of $J = 1, 2$, and 3, respectively. Fig. 5(b) shows a reduction in the MHD as J increases, which demonstrates the advantage of using more identification codewords for each EU. Furthermore, we highlight the case of $J = 3$ with $\Delta_z = 10^{-2}$, in which our proposed MHD-optimal algorithm achieves exact estimation of the active users using a limited number of measurements ($R = 0.2$).

VII. CONCLUSION

In this paper, we studied the MMV signal estimation problem with user-defined additive error metrics on the estimate. We proposed an algorithmic framework that is optimal under arbitrary additive error metrics and verified its optimality. As examples, we derived algorithms that yield the optimal estimates in the sense of mean weighted support set error and mean absolute error, respectively. Numerical results not only verified the theoretic performance but also verified the intuition that having more signal vectors in MMV problems is beneficial to the estimation algorithm. We further provided simulation results for active user detection problem in multi-user communication systems, which is a real-world application of MMV models with the goal of minimizing the Hamming distance. Simulation results demonstrated the promise of our algorithm.

⁵Details can be found in Krzakala et al. [21] and Barbier and Krzakala [25].

⁶Note that the entries of the signal estimated by OMP are not exactly 0's and 1's. Hence, in order to provide meaningful results, we threshold the OMP estimates before calculating the Hamming distance.

APPENDIX

A. Derivation of g_{out} for logistic channels (7)

Byrne and Schniter [26] provide a method to derive g_{out} for logistic channels (7), but the actual formula for g_{out} is not given in their paper. To make our paper self-contained, we outline the derivation of g_{out} for logistic channels. In order to calculate $g_{out}(k, y, \Theta)$ (4), we need to find $f(w|k, y, \Theta)$ (5) and calculate $\mathbb{E}[w|k, y, \Theta]$. For logistic channels (7),

$$f(w|k, y, \Theta) = \frac{1}{\tilde{Z}} \times \left[\frac{\delta(y-1)}{1+e^{-w}} + \delta(y) \frac{e^{-w}}{1+e^{-w}} \right] \frac{1}{\sqrt{2\pi\Theta}} e^{-\frac{1}{2\Theta}(w-k)^2}, \quad (25)$$

where \tilde{Z} is a normalization factor. Therefore, it is difficult to calculate $\mathbb{E}[w|k, y, \Theta]$. Instead of calculating $\mathbb{E}[w|k, y, \Theta]$ by brute force, Byrne and Schniter [26] use a mixture of Gaussian cumulative distribution functions (CDF's) to approximate the sigmoid function $\frac{1}{1+\exp(-aw)} \approx \sum_{u=1}^{u_{\max}} \alpha_u \Phi(\frac{w}{\sigma_u/a})$ [34], where u_{\max} is the maximum number of Gaussian CDF's one wants to use, $\Phi(\frac{w}{\sigma_u/a})$ denotes the Gaussian CDF whose standard deviation is $\frac{\sigma_u}{a}$, and α_u is the weight.

Following Byrne and Schniter [26], we define the i -th moment

$$\int w^i \mathcal{N}(w; k, \Theta) \Phi\left(\frac{w}{\sigma_u/a}\right) dz = T_i(u), \quad (26)$$

where $\mathcal{N}(w; k, \Theta)$ is the pdf of an RV w with mean k and variance Θ , and $\Phi(\cdot)$ is the CDF of a standard Gaussian RV. Defining $\eta_u = \frac{k}{\sqrt{(\frac{\sigma_u}{a})^2 + \Theta}}$, we obtain

$$T_0(u) = \Phi(\eta_u), \quad (27)$$

$$T_1(u) = k\Phi(\eta_u) + \frac{\Theta\phi(\eta_u)}{\sqrt{(\frac{\sigma_u}{a})^2 + \Theta}}, \quad (28)$$

$$T_2(u) = \frac{(T_1(u))^2}{\Phi(\eta_u)} + \Theta\Phi(\eta_u) - \frac{\Theta^2\phi(\eta_u)}{(\frac{\sigma_u}{a})^2 + \Theta} \left(\eta_u + \frac{\phi(\eta_u)}{\Phi(\eta_u)} \right), \quad (29)$$

where $\phi(\eta_u)$ is the pdf of a standard Gaussian RV at η_u . Hence, the normalization factor \tilde{Z} in (25) can be derived,

$$\begin{aligned} \tilde{Z} &= \int \left[\frac{\delta(y-1)}{1+e^{-aw}} + \delta(y) \frac{e^{-aw}}{1+e^{-aw}} \right] \frac{e^{-\frac{1}{2\Theta}(w-k)^2}}{\sqrt{2\pi\Theta}} dz \\ &= \begin{cases} \sum_{u=1}^{u_{\max}} \alpha_u \Phi(\eta_u), & y = 1, \\ 1 - \sum_{u=1}^{u_{\max}} \alpha_u \Phi(\eta_u), & y = 0. \end{cases} \end{aligned} \quad (31)$$

We can further obtain the expression for $\mathbb{E}[w|k, y, \Theta]$ in (32). Hence, we can calculate g_{out} (4).

Apart from g_{out} , we also need to find the partial derivative of g_{out} (33), which according to Rangan [20] satisfies

$$-\frac{\partial}{\partial k} g_{out}(k, y, \Theta) = \frac{1}{\Theta} \left(1 - \frac{\text{var}(w|k, y, \Theta)}{\Theta} \right), \quad (33)$$

where $\text{var}(w|k, y, \Theta) = \mathbb{E}[w^2|k, y, \Theta] - [\mathbb{E}[w|k, y, \Theta]]^2$. Note

that $\mathbb{E}[w^2|k, y, \Theta]$ can be derived in the same way as (32) and the result is given below,

$$\mathbb{E}[w^2|k, y, \Theta] = \begin{cases} k^2 + \Theta + \frac{\sum_{u=1}^{u_{\max}} \alpha_u \xi_u}{\sum_{u=1}^{u_{\max}} \alpha_u \Phi(\eta_u)}, & y = 1, \\ k^2 + \Theta - \frac{\sum_{u=1}^{u_{\max}} \alpha_u \xi_u}{1 - \sum_{u=1}^{u_{\max}} \alpha_u \Phi(\eta_u)}, & y = 0, \end{cases} \quad (34)$$

where

$$\xi_u = \frac{2k\Theta\phi(\eta_u)}{\sqrt{(\frac{\sigma_u}{a})^2 + \Theta}} - \frac{\Theta^2\eta_u\phi(\eta_u)}{(\frac{\sigma_u}{a})^2 + \Theta}. \quad (35)$$

B. Inverting the MMSE

For the MMV problem with i.i.d. matrices and joint Bernoulli-Gaussian signals, Zhu et al. provide an information-theoretic characterization of the MMSE by using replica analysis [12]. Suppose that we have already obtained the MMSE for an MMV problem. This appendix briefly shows how to invert the MMSE expression in order to obtain the equivalent scalar channel noise variance Δ_v .

The optimal denoiser for the pseudo data is $\tilde{\mathbf{x}}_n = \mathbb{E}[\mathbf{x}_n|\mathbf{q}_n] = f_{a_n}(\Delta_v, \mathbf{q}_n)$, where $f_{a_n}(\Delta_v, \mathbf{q}_n)$ is given in (8). We then express MMSE expression using $\mathbb{E}[\mathbf{x}_n|\mathbf{q}_n]$ as follows,

$$\text{MMSE} = \mathbb{E}[(\tilde{\mathbf{x}}_n - \mathbf{x}_n)^2] = J\rho - \mathbb{E}[(\mathbb{E}[\mathbf{x}_n|\mathbf{q}_n])^2]. \quad (36)$$

We calculate $\mathbb{E}[(\mathbb{E}[\mathbf{x}_n|\mathbf{q}_n])^2]$ in (37), where the J -dimensional integral can be simplified by a change of coordinates. Then, we plug (37) into (36), and express the MMSE as a function of Δ_v . Finally, we numerically solve Δ_v for any given MMSE.

ACKNOWLEDGMENTS

We would like to thank Jin Tan for providing valuable insights into achieving metric-optimal performance in signal estimation. Jong Chul Ye, Yavuz Yapici, and Ismail Guvenc helped us identify some real-world applications for minimizing error metrics that are different from the MSE.

REFERENCES

- [1] J. Chen and X. Huo, "Theoretical results on sparse representations of multiple measurement vectors," *IEEE Trans. Signal Process.*, vol. 54, no. 12, pp. 4634–4643, Dec. 2006.
- [2] S. F. Cotter, B. D. Rao, K. Egan, and K. Kreutz-Delgado, "Sparse solutions to linear inverse problems with multiple measurement vectors," *IEEE Trans. Signal Process.*, vol. 53, no. 7, pp. 2477–2488, July 2005.
- [3] M. Mishali and Y. C. Eldar, "Reduce and boost: Recovering arbitrary sets of jointly sparse vectors," *IEEE Trans. Signal Process.*, vol. 56, no. 10, pp. 4692–4702, Oct. 2009.
- [4] E. Berg and M. P. Friedlander, "Joint-sparse recovery from multiple measurements," *Arxiv preprint arXiv:0904.2051*, Apr. 2009.

$$\mathbb{E}[w|k, y, \Theta] = \begin{cases} \frac{1}{\bar{Z}} \int \frac{w}{1 + e^{-aw}} \frac{e^{-\frac{1}{2\Theta}(w-k)^2}}{\sqrt{2\pi\Theta}} dz = \frac{\sum_{u=1}^{u_{\max}} \alpha_u T_1(u)}{\sum_{u=1}^{u_{\max}} \alpha_u T_0(u)} = k + \frac{\Theta \sum_{u=1}^{u_{\max}} \frac{\alpha_u \phi(\eta_u)}{\sqrt{(\frac{\sigma_u}{a})^2 + \Theta}}}{\sum_{u=1}^{u_{\max}} \alpha_u \Phi(\eta_u)}, & y = 1, \\ \frac{1}{\bar{Z}} \int \frac{w e^{-aw}}{1 + e^{-aw}} \frac{e^{-\frac{1}{2\Theta}(w-k)^2}}{\sqrt{2\pi\Theta}} dz = \frac{k - \sum_{u=1}^{u_{\max}} \alpha_u T_1(u)}{1 - \sum_{u=1}^{u_{\max}} \alpha_u T_0(u)} = k - \frac{\Theta \sum_{u=1}^{u_{\max}} \frac{\alpha_u \phi(\eta_u)}{\sqrt{(\frac{\sigma_u}{a})^2 + \Theta}}}{1 - \sum_{u=1}^{u_{\max}} \alpha_u \Phi(\eta_u)}, & y = 0. \end{cases} \quad (32)$$

$$\begin{aligned} \mathbb{E}[(\mathbb{E}[\mathbf{x}_n | \mathbf{q}_n])^2] &= \int_{\mathbf{q}_n} f(\mathbf{q}_n) (\mathbb{E}[\mathbf{x}_n | \mathbf{q}_n])^2 d\mathbf{q}_n \\ &= \frac{\left(\frac{\rho}{1+\Delta_v}\right)^2}{[2\pi(1+\Delta_v)]^{J/2}} \int_{\mathbf{q}_n} \frac{\mathbf{q}_n \mathbf{q}_n^T}{\rho \exp\left[\frac{\mathbf{q}_n \mathbf{q}_n^T}{2(1+\Delta_v)}\right] + (1-\rho) \left(1 + \frac{1}{\Delta_v}\right)^{J/2} \exp\left[\frac{\mathbf{q}_n \mathbf{q}_n^T (\Delta_v - 1)}{2\Delta_v(1+\Delta_v)}\right]} d\mathbf{q}_n. \end{aligned} \quad (37)$$

- [5] O. Lee, J. M. Kim, Y. Bresler, and J. C. Ye, "Compressive diffuse optical tomography: Noniterative exact reconstruction using joint sparsity," *IEEE Trans. Medical Imaging*, vol. 30, no. 5, pp. 1129–1142, May 2011.
- [6] K. Lee, Y. Bresler, and M. Junge, "Subspace methods for joint sparse recovery," *IEEE Trans. Inf. Theory*, vol. 58, no. 6, pp. 3613–3641, June 2012.
- [7] J. C. Ye, J. M. Kim, and Y. Bresler, "Improving M-SBL for joint sparse recovery using a subspace penalty," *IEEE Trans. Signal Process.*, vol. 63, no. 24, pp. 6595–6605, Dec. 2015.
- [8] H. Jung, J. C. Ye, and E. Y. Kim, "Improved k-t BLAST and k-t SENSE using FOCUSS," *Physics in Medicine and Biology*, vol. 52, no. 11, pp. 3201–3226, May 2007.
- [9] H. Jung, K. Sung, K. S. Nayak, E. Y. Kim, and J. C. Ye, "k-t FOCUSS: A general compressed sensing framework for high resolution dynamic MRI," *J. Magnetic Resonance in Medicine*, vol. 61, no. 1, pp. 103–116, Jan. 2009.
- [10] V. Boljanović, D. Vukobratović, P. Popovski, and Č. Stefanović, "User activity detection in massive random access: Compressed sensing vs. coded slotted ALOHA," *Arxiv preprint arXiv:1706.09918v1*, June 2017.
- [11] M. F. Duarte, M. B. Wakin, D. Baron, S. Sarvotham, and R. G. Baraniuk, "Measurement bounds for sparse signal ensembles via graphical models," *IEEE Trans. Inf. Theory*, vol. 59, no. 7, pp. 4280–4289, July 2013.
- [12] J. Zhu, D. Baron, and F. Krzakala, "Performance limits for noisy multimeasurement vector problems," *IEEE Trans. Signal Process.*, vol. 65, no. 9, pp. 2444–2454, May 2017.
- [13] J. Zhu, *Statistical Physics and Information Theory Perspectives on Linear Inverse Problems*, Ph.D. thesis, North Carolina State University, Raleigh, NC, Jan. 2017.
- [14] J. A. Tropp, A. C. Gilbert, and M. J. Strauss, "Algorithms for simultaneous sparse approximation. Part I: Greedy pursuit," *Signal Process.*, vol. 86, no. 3, pp. 572–588, Mar. 2006.
- [15] D. Malioutov, M. Cetin, and A. S. Willsky, "A sparse signal reconstruction perspective for source localization with sensor arrays," *IEEE Trans. Signal Process.*, vol. 53, no. 8, pp. 3010–3022, Aug. 2005.
- [16] J. A. Tropp, "Algorithms for simultaneous sparse approximation. Part II: Convex relaxation," *Signal Process.*, vol. 86, no. 3, pp. 589–602, Mar. 2006.
- [17] J. Ziniel and P. Schniter, "Efficient message passing-based inference in the multiple measurement vector problem," in *Proc. IEEE Asilomar Conf. Signals, Syst., and Comput.*, Nov. 2011, pp. 1447–1451.
- [18] J. Tan, D. Carmon, and D. Baron, "Optimal estimation with arbitrary error metric in compressed sensing," in *Proc. IEEE Stat. Signal Process. Workshop (SSP)*, Aug. 2012, pp. 588–591.
- [19] J. Tan, D. Carmon, and D. Baron, "Signal estimation with additive error metrics in compressed sensing," *IEEE Trans. Inf. Theory*, vol. 60, no. 1, pp. 150–158, Jan. 2014.
- [20] S. Rangan, "Generalized approximate message passing for estimation with random linear mixing," in *Proc. IEEE Int. Symp. Inf. Theory (ISIT)*, St. Petersburg, Russia, July 2011, pp. 2168–2172.
- [21] F. Krzakala, M. Mézard, F. Sausset, Y. Sun, and L. Zdeborová, "Probabilistic reconstruction in compressed sensing: Algorithms, phase diagrams, and threshold achieving matrices," *J. Stat. Mech. – Theory E.*, vol. 2012, no. 08, pp. P08009, Aug. 2012.
- [22] D. Baron, M. B. Wakin, M. F. Duarte, S. Sarvotham, and R. G. Baraniuk, "Distributed compressed sensing," Tech. Rep. ECE-0612, Rice University, Dec. 2006.
- [23] J. Ziniel and P. Schniter, "Efficient high-dimensional inference in the multiple measurement vector problem," *IEEE Trans. Signal Process.*, vol. 61, no. 2, pp. 340–354, Jan. 2013.
- [24] D. Guo and C. C. Wang, "Multiuser detection of sparsely spread CDMA," *IEEE J. Sel. Areas Commun.*, vol. 26, no. 3, pp. 421–431, Apr. 2008.
- [25] J. Barbier and F. Krzakala, "Approximate message-passing decoder and capacity-achieving sparse superposition codes," *IEEE Trans. Inf. Theory*, vol. 63, no. 8, pp. 4894–4927, Aug. 2017.
- [26] E. Byrne and P. Schniter, "Sparse multinomial logistic regression via approximate message passing," *Arxiv preprint arXiv:1509.04491*, Sept. 2015.
- [27] G. Hannak, A. Perelli, N. Goertz, G. Matz, and M. E. Davies, "Performance analysis of approximate message passing for distributed compressed sensing," *Arxiv preprint arXiv:1712.04893v1*, Dec. 2017.
- [28] T. M. Cover and J. A. Thomas, *Elements of Information Theory*, New York, NY, USA: Wiley-Interscience, 2006.
- [29] J. Zhu and D. Baron, "Performance regions in compressed sensing from noisy measurements," in *Proc. IEEE Conf. Inf. Sci. Syst. (CISS)*, Baltimore, MD, Mar. 2013.
- [30] D. Donoho, "Compressed sensing," *IEEE Trans. Inf. Theory*, vol. 52, no. 4, pp. 1289–1306, Apr. 2006.
- [31] E. Candès, J. Romberg, and T. Tao, "Robust uncertainty principles: Exact signal reconstruction from highly incomplete frequency information," *IEEE Trans. Inf. Theory*, vol. 52, no. 2, pp. 489–509, Feb. 2006.
- [32] R. G. Baraniuk, "A lecture on compressive sensing," *IEEE Signal Process. Mag.*, vol. 24, no. 4, pp. 118–121, July 2007.
- [33] Y. C. Pati, R. Rezaifar, and P. S. Krishnaprasad, "Orthogonal matching pursuit: Recursive function approximation with applications to wavelet decomposition," *Proc. 27th Asilomar Conf. Signals, Syst. Comput.*, pp. 40–44, Nov. 1993.
- [34] L. Stefanski, "A normal scale mixture representation of the logistic distribution," *Stat. Prob. Lett.*, vol. 11, no. 1, pp. 67–70, 1991.